CrossMark

Humidity-sensing properties of hierarchical ZnO/MWCNTs/ZnO nanocomposite film sensor based on electrostatic layer-by-layer self-assembly

Dongzhi Zhang[1] · Nailiang Yin[1] · Bokai Xia[1] · Yan Sun[1] · Yifan Liao[2] ·
Zilan He[2] · Shuang Hao[2]

Abstract This paper demonstrated a resistive-type humidity sensor with hierarchical ZnO/MWCNTs/ZnO nanocomposite film coated. Hydrothermally synthesized ZnO nanorods and functionalized multi-walled carbon nanotubes (MWCNTs) were utilized to construct a humidity sensor by using electrostatic layer-by-layer (ELbL) self-assembly technique. The characterization results including scanning electron microscope and X-ray diffraction confirmed the successful formation of as-prepared nanostructures. The electrical properties of the sensing films were investigated under different deposition time in the ELbL self-assembly process. The humidity sensing behaviors of the ZnO/MWCNTs/ZnO hierarchical hybrid film were investigated in a wide relative humidity (RH) range. It is found that the sensor exhibited an excellent linear response with RH, small hysteresis, acceptable repeatability and swift response-recovery characteristics. The possible sensing mechanism for the presented sensor was attributed to the nanostructure of ZnO/MWCNTs/ZnO and swelling effects between interlayers. This study provided a benchmark for humidity sensor fabrication using ELbL self-assembly technique.

✉ Dongzhi Zhang
dzzhang@upc.edu.cn

[1] College of Information and Control Engineering, China University of Petroleum (East China), Qingdao 266580, People's Republic of China

[2] Electric Power Research Institute, CSG, Guangzhou 510080, People's Republic of China

1 Introduction

Measurement of relative humidity (RH) is playing an increasingly essential part in many fields, such as agriculture, biological, environmental monitoring and meteorological services. Portable, reliable and low-cost humidity sensors are greatly desired and appreciated, and many methods have been devoted to developing practical humidity sensors, such as bulk acoustic wave (BAW) [1], surface acoustic wave (SAW) [2, 3], quartz crystal microbalance (QCM) [4–8], and field-effect transistor (FET) [9, 10]. Notably, metal oxide (MOx) semiconductors are widely used for making low-cost gas sensors, due to their electrical conductivity changes depend upon the humidity surrounding them [11, 12]. ZnO as a typical n-type MOx, has been widely investigated due to its excellent properties, such as nano-size, stable physical and chemical properties [13, 14]. Up to now, ZnO materials have been successfully used as sensing materials for detecting ethanol, toluene, and humidity by converting the information in relation with gas type and concentration into electrical signals when exposed to different gases [15, 16]. However, the gas sensors fabricated with pure metal oxide have some drawbacks including low sensitivity, long response and recovery times and high operation temperature [17–19].

Carbon nanotubes (CNTs) are one of the most important one-dimensional nanomaterials in nature which are attracting extensive attention all over the world [20–22]. Nowadays, CNTs have been used in a broad spectrum of various fields, such as super capacitor, solar cells, catalyst support, hydrogen storage, and gas sensors [23–27]. However, Adjizian et al. [18] found that pristine multi-walled carbon nanotubes (MWCNTs) showed very long response and recovery time to RH, e.g., the recovery time

was 2.5 h for the sensor even operated at 150 °C. Yoo et al. [20] prepared a resistive-type humidity sensor based on MWCNTs/polyimide composite film and found that its resistance changed linearly with RH variation, but the sensitivity was only 0.0047/% RH. Therefore, high-reliable, low-cost and high-sensitive humidity sensors are greatly required in environment monitoring and other versatile applications.

In this work, we fabricated a resistive-type humidity sensor with hierarchical ZnO/MWCNTs/ZnO nanocomposite film by using electrostatic layer-by-layer (ELbL) self-assembly method. The sensing film was characterized by scanning electron microscope (SEM) and X-ray diffraction (XRD). The humidity-sensing properties of the ZnO/MWCNTs/ZnO hybrid film were investigated at room temperature under exposure of various RH levels. The proposed sensor exhibited high response to humidity, short response and recovery time, small hysteresis and acceptable repeatability. Furthermore, the possible sensing mechanism for the presented sensor was discussed in this paper.

2 Experiment

2.1 Materials

Pristine MWCNTs (10–30 μm in length, 20–30 nm in diameter) were chemically functionalized with the concentrated acid (3:1 for 98 wt% H_2SO_4:70 wt% HNO_3) at 110 °C and stirred at 140 r/min for 1 h, followed by filtering and several rinsing using de-ionized water (DI water) until the supernatant had pH value of 5 or more. The chemically functionalized MWCNTs were negatively charged by covalently-attached carboxylic groups on the sidewalls as well as openings, which facilitated the uniformly well-dispersion of MWCNTs into DI water. Zinc nitrate hexahydrate $Zn(NO_3)_2 \cdot 6H_2O$ and NaOH was purchased from Sinopharm Chemical Reagent Co. Ltd. Polyelectrolytes used for LbL assembly were 1.5 wt% poly(diallyldimethylammonium chloride) [PDDA (Sigma-Aldrich Inc.), molecular weight (MW) of 200–350 K, polycation] at pH 7.5 and 0.3 wt% poly(sodium 4-styrenesulfonate) [PSS (Sigma-Aldrich Inc.), MW of 70 K, polyanion] at pH 6.5 with 5 M NaCl in both for better surface coverage.

2.2 Fabrication

The structure of the humidity sensor is shown in Fig. 1. The sensor was fabricated on a polyimide (PI) substrate by using microfabrication technology. Two coil-like electrodes are used as interdigital electrodes (IDE). The sensing
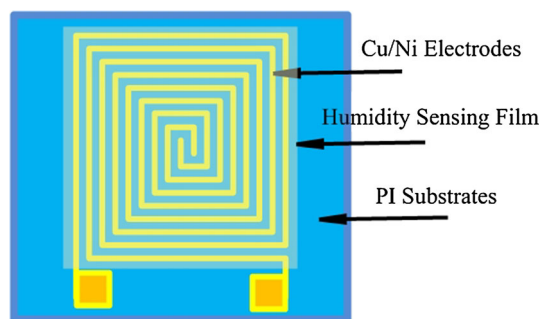

Fig. 1 Structure illustration of the humidity sensor

film of hierarchical ZnO/MWCNTs/ZnO nanostructure was fabricated by the combination of hydrothermal synthesis and electrostatic layer-by-layer (ELbL) self-assembly technique, as shown in Fig. 2. In the typical process, the first step was the synthesis of ZnO nanorods by using a hydrothermal route. 2.08 g $Zn(NO_3)_2 \cdot 6H_2O$ was dissolved into 140 mL deionized (DI) water with stirring for 1 h, and 20 mL of NaOH (4 mol/L) was added into the resulting solution with stirring for 30 min. And then, the obtained solution was transferred into a 200 mL stainless-steel autoclave and heated in an oven at 120 °C for 12 h. Afterward, the final product of ZnO suspension was washed with DI water and anhydrous ethanol for several times to remove excess ions, and subsequent was ultrasonicated for 1 h and centrifugated for 15 min. The second step is the ELbL self-assembly process for fabricating ZnO/MWCNTs/ZnO. Two bi-layers of PDDA/PSS were firstly self-assembled as precursor layers for charge enhancement, and then three self-assembled monolayers (SAMs) of ZnO/MWCNTs/ZnO were deposited through the alternative immersion into suspensions of ZnO and MWCNTs. Intermediate rinsing with DI water and drying with nitrogen flow were required after each monolayer assembly to reinforce the interconnection between layers. The immersing time here used was 10 min for polyelectrolytes, 15 min for MWCNTs, 10, 25, 40 and 55 min was selected for ZnO, respectively, and a serial of ZnO/MWCNTs/ZnO samples were prepared and designated as S_1, S_2, S_3 and S_4 for making comparison. Afterward, the self-assembled ZnO/MWCNTs/ZnO samples were dried in the oven at 50 °C for 3 h.

2.3 Instrument and analysis

The surface microscope of MWCNTs, ZnO nanorods, and self-assembled ZnO/MWCNTs/ZnO films was measured with field emission scanning electron microscopy (FESEM, Hitachi S-4800). And their XRD analyses were performed by the X-ray diffractometer (Rigaku D/Max 2500PC,

Fig. 2 Fabrication of **a** ZnO suspension by hydrothermal route and **b** ZnO/MWCNTs/ZnO nanocomposite film via ELbL self-assembly approach
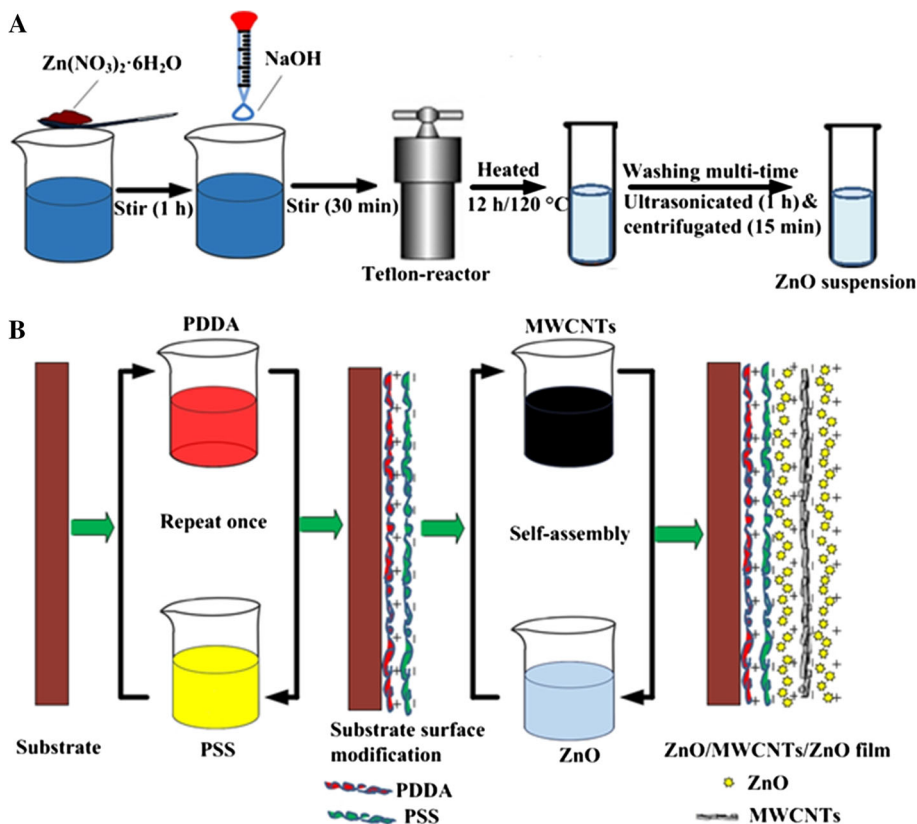
Japan) using Cu Kα radiation with a wavelength of 1.5418 Å.

The humidity sensing properties were investigated by exposing the ZnO/MWCNTs/ZnO film sensor to various RH levels, which were achieved by several saturated aqueous solutions according to our previously reported publication [28]. Saturated solutions of LiCl, CH$_3$COOK, MgCl$_2$, K$_2$CO$_3$, Mg(NO$_3$)$_2$, CuCl$_2$, NaCl, KCl and K$_2$SO$_4$ in a closed vessel were used to yield approximately 11, 23, 33, 43, 52, 67, 75, 85 and 97 % RH levels, respectively. The film resistance of the sensor was recorded using a data logger (Agilent 34970A). P$_2$O$_5$ powder was used for the release of water molecules. The figures of merit used for evaluating the sensor performance are the normalized response (Nr) and sensitivity (S), determined by $Nr = \Delta R/R_0 = (R_{RH} - R_0)/R_0 \times 100~\%$ and $S = \Delta R/\Delta RH$, respectively, where R_{RH} and R_0 are the electrical resistance of the sensor in the given RH and dry air, respectively.

3 Results and discussion

## 3.1 SEM and XRD characterization

Figure 3 shows the observed SEM and XRD characterization of MWCNTs, ZnO, ZnO/MWCNTs/ZnO film. The

result in Fig. 3a indicates interweaved MWCNTs with a random network structure. Figure 3b shows the ZnO sample was nanorod-shaped crystalline. Figure 3c illustrates the self-assembled ZnO/MWCNTs/ZnO film is constructed by ZnO nanorods and MWCNTs wrapped closely together. Figure 3d plots the XRD spectrum for MWCNTs, ZnO and ZnO/MWCNTs/ZnO film. XRD pattern of ZnO nanorods shows polycrystalline structure with major peaks in the direction (1 0 0), (0 0 2) and (1 0 1). The main feature of the diffraction peaks are observed at 2θ angle of 25.9° and 24.6° for MWCNTs and ZnO/MWCNTs/ZnO film, respectively. According to the Bragg formula, the interlayer distance of the MWCNTs film can be determined as 3.44 Å, as well we find that the interlayer distance of the ZnO/MWCNTs/ZnO film is 3.61 Å, which is larger than that of MWCNTs film due to the surface of ZnO/MWCNTs/ZnO film is rougher than that of MWCNTs.

3.2 Electrical properties of samples

The electrical properties of self-assembled five samples were investigated upon different deposition times. Figure 4 shows the film resistance as a function of deposition time for ZnO SAM. The fitting equation for film resistance Y (Ω) as a function of deposition time X (min) can be

Fig. 3 SEM characterization of **a** MWCNTs, **b** ZnO nanorods, **c** ZnO/MWCNTs/ZnO nanocomposite and **d** XRD spectrum for MWCNTs, ZnO and ZnO/MWCNTs/ZnO nanocomposite film
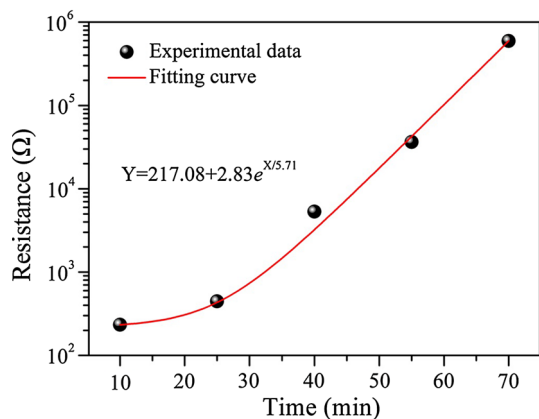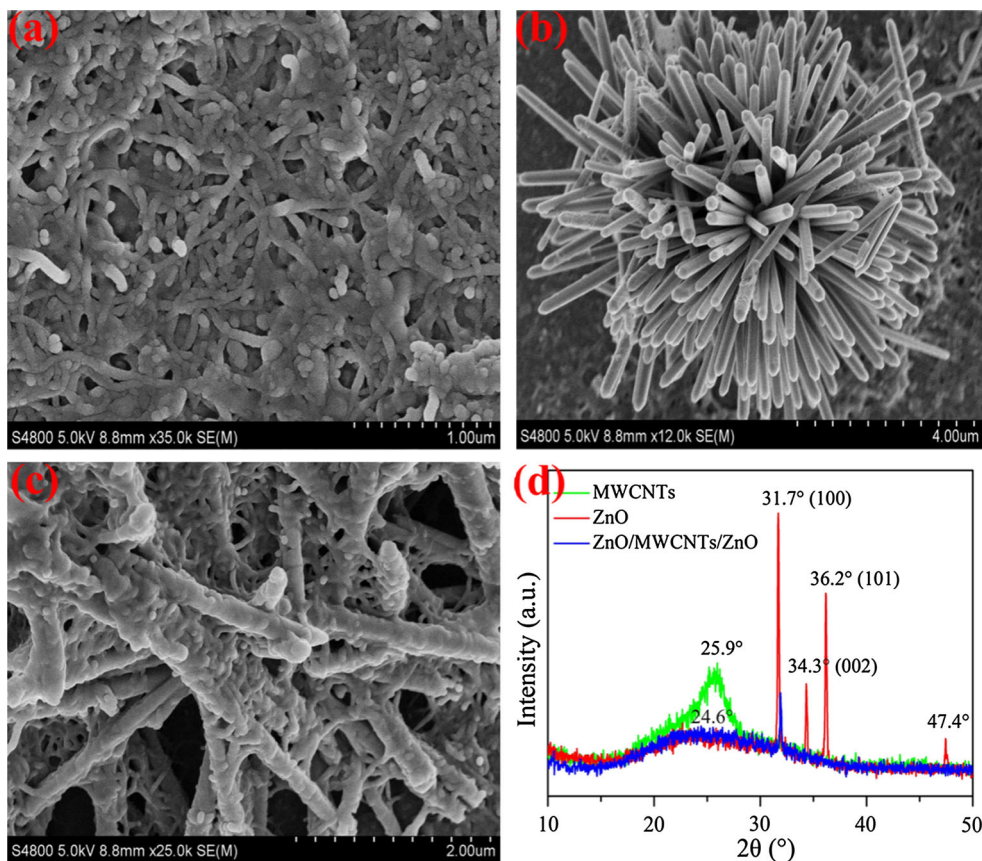

Fig. 4 Film resistance as a function of deposition time for ZnO SAM

represented as $Y = 217.08 + 2.83e^{X/5.71}$. The film resistance is exponentially increased with the rising of deposition time. As well known, MWCNTs have a better conductivity than that of ZnO, and the amount of ZnO in the ZnO/MWCNTs/ZnO nanocomposite is increased as the increasing of the deposition time, and hence leads to an increase in film resistance. It is found that the tunable electrical properties of ZnO/MWCNTs/ZnO nanocomposite can be achieved via different deposition time for ZnO SAM.
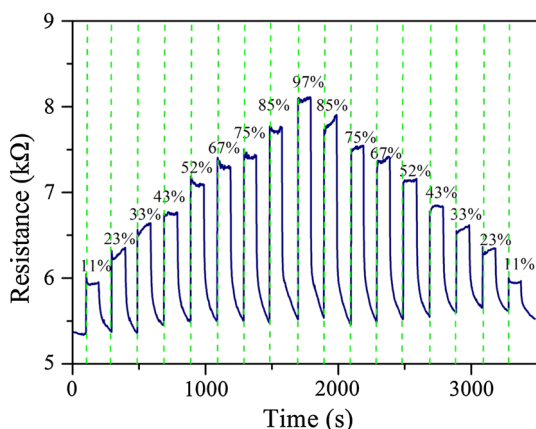
3.3 Humidity-sensing behaviors

The effect of deposition time of ZnO SAM on the humidity sensing performance of ZnO/MWCNTs/ZnO nanocomposite was examined. Figure 5 shows the response curves of the four ZnO/MWCNTs/ZnO samples exposed to different RH at room temperature. The deposition times of ZnO SAM for the four samples were 10, 25, 40 and
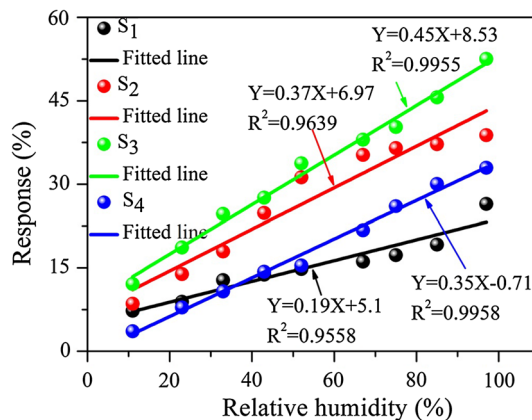
Fig. 5 Relationship between response and relative humidity of four different samples

55 min, respectively. A good linearity of the sensor response as a function of RH is observed for the four samples. The fitting equation of the four samples for response Y and relative humidity (RH) X can be represented as $Y = 0.19X + 5.1$, $Y = 0.37X + 6.97$, $Y = 0.45X + 8.53$ and $Y = 0.35X - 0.71$, and the linear regression coefficient, R^2, is 0.9558, 0.9639, 0.9955 and 0.9958, respectively. As the increasing of the deposition time of ZnO SAM, the sensor response increases and reaches a maximum value for the sensor S_3 with 40 min, then decreases with further increasing the deposition time to 55 min. It can be observed that the sensor S_4 with deposition time of 55 min for ZnO SAM exhibits lower sensing response due to the increased benchmark resistance of the hybrid film with increasing content of ZnO nanorods, leading to a decreased response in sensor properties. Thus, the following sensing measurements are performed using S_3 as sensing material.

Figure 6 shows the resistance measurement of the sensor sample of S_3 exposed to various RH levels. The switching RH test is performed through exposure/recovery cycles under different RH environments between 0 and 11, 23, 33, 43, 52, 67, 75, 85, 97 % RH, and then conversely from high RH to low RH. A clear increase in the sensor resistance is observed with the rising of RH in a large range of 11–97 %, and the corresponding normalized response values are calculated to be 12.1, 18.64, 24.66, 27.59, 33.76, 38.01, 40.29, 45.61, 52.53 % when the sensor exposed to 11, 23, 33, 43, 52, 67, 75, 85, 97 % RH. The measured resistance of the sensor is ranging of 5.94–8.10 kΩ in a wide RH of 11–97 % with a sensitivity of 24.8 Ω/% RH, which is much higher than the sensitivity of other previously reported pure MWCNT humidity sensor (~2.3 Ω/% RH) [29, 30]. Furthermore, the presented sensor overcomes the limit of high resistance (hundreds of MΩ) in practical applications of pure ZnO humidity sensor [31, 32]. We also measured the hysteresis of the presented sensor through the comparison of RH-increasing for water molecules absorption and RH-decreasing for water molecules desorption with RH ranging from 11 to 97 %, the maximum hysteresis was about 2.02 % occurred at 75 % RH, as shown in Fig. 7.

Figure 8 shows the repeatability of ZnO/MWCNTs/ZnO film sensor performed under the same experimental conditions. The repeatability characteristics is measured for five exposure/recovery cycles repeatedly for 33, 67 and 97 % RH. The film humidity sensor exhibited a clear response-recovery behavior and acceptable repeatability for humidity sensing. Figure 9 demonstrates the time-dependent response and recovery curves of the sensor to a RH pulse from 0 to 97 % RH, respectively. The time taken by a sensor to achieve 90 % of the total resistance change is defined as the response or recovery time [33]. Response time and recovery time of ~4 and 34–74 s are observed, respectively, better than that of conventional humidity sensors [34–36].

The above experimental results demonstrated that proposed film sensor is very sensitive toward RH, highlighting the ZnO/MWCNTs/ZnO nanocomposite is an excellent candidate material for constructing humidity sensors. To explain the above observed results, the possible humidity sensing mechanism for the presented sensor may attribute to the nanostructure of ZnO/MWCNTs/ZnO and swelling effects between interlayers. At low RH, the electron transport through ZnO/MWCNTs/ZnO film exhibits p-type semiconducting behavior and is dominated by positive charge carriers (holes), whereas the adsorbed water molecules on the sensing film surface serves as electron donors [37, 38]. The chemisorbed water molecules cause a reduction of hole, resulting in the increase of film resistance. At high RH, the adsorbed water molecules enter into the multi-layer film can lead to an interlayer swelling effect occurs. The swelling of the ZnO/MWCNTs/ZnO increases

Fig. 6 Resistance response of the ZnO/MWCNTs/ZnO film sensor under switching RH
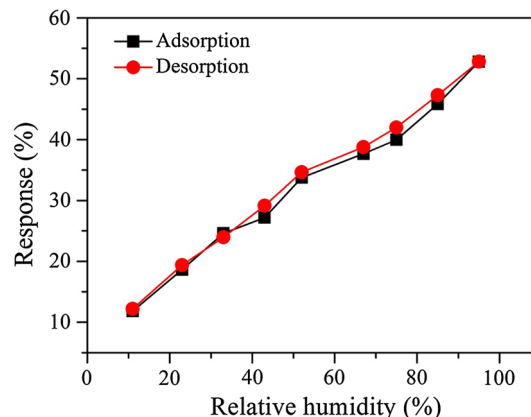
Fig. 7 Hysteresis of the proposed sensor under different RH
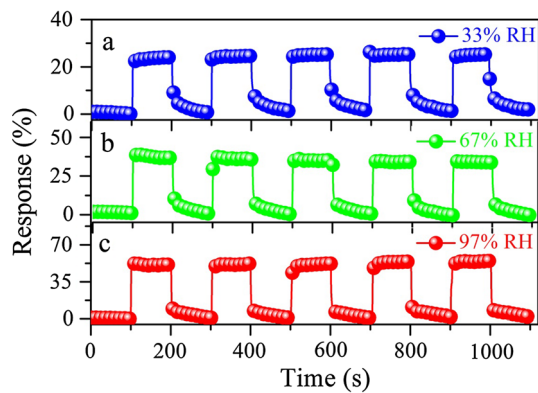
Fig. 8 Repeatability of the ZnO/MWCNTs/ZnO film sensor for *a* 33 %, *b* 67 % and *c* 97 % RH at room temperature
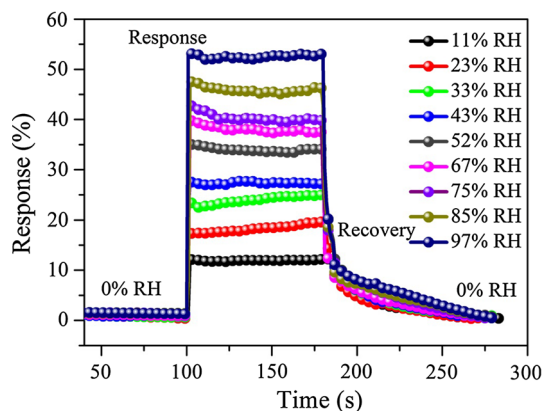
Fig. 9 Typical response and recovery curves of the ZnO/MWCNTs/ZnO film sensor to a RH pulse between 0 and 97 % RH, respectively

their interlayer distance largely and deteriorates the degree of connectivity in the ELbL self-assembled nanocomposite film, resulting in an increase of sensor resistance [39, 40]. Based on the discussion above, we can consider that the major sensing mechanism is attributed to the p-type semiconducting behavior at low RH, and the interlayer swelling of ZnO/MWCNTs/ZnO film at high RH.

4 Conclusions

A humidity sensor based on hierarchical ZnO/MWCNTs/ZnO nanocomposite was presented in this paper. The humidity sensor was fabricated on a polyimide substrate by using ELbL self-assembly technology. SEM and XRD measurements were used to confirm the preparation of ZnO nanorods and functionalized-MWCNTs. The humidity sensing behaviors of the presented sensor were investigated under exposure toward different RH levels ranging of 11–97 % RH. The experiment results showed the sensor has high response to humidity, short response and recovery

time, small hysteresis and acceptable repeatability, highlighting the ZnO/MWCNTs/ZnO hierarchical nanocomposite is an excellent candidate material for constructing humidity sensors.

Compliance with ethical standards

Conflict of interest The authors declared that they have no conflicts of interest to this work.

References

1. X.T. Qiu, R. Tang, J. Zhu, J. Oiler, C.J. Yu, Z.Y. Wang, H.U. Yu, The effects of temperature, relative humidity and reducing gases on the ultraviolet response of ZnO based film bulk acoustic-wave resonator. Sens. Actuators, B **151**, 360–364 (2011)
2. C.M. Lin, Y.Y. Chen, V. Felmetsger, T. Riekkinen, D. Senesky, A. Pisaon, Surface acoustic wave devices on AlN/3C-SiC/Si multilayer structures. J. Micromech. Microeng. **23**, 025019 (2013)
3. A. Buvailo, Y.J. Xing, J. Hines, E. Borguet, Thin polymer film based rapid surface acoustic wave humidity sensors. Sens. Actuators, B **156**, 444–449 (2011)
4. Y. Zhu, J.C. Chen, H.M. Li, Y.H. Zhu, J.Q. Xu, Synthesis of mesoporous SnO₂–SiO₂ composites and their application as quartz crystal microbalance humidity sensor. Sens. Actuators, B **193**, 320–325 (2014)
5. Y. Yao, X.D. Chen, X.Y. Li, X.P. Chen, N. Li, Investigation of the stability of QCM humidity sensor using graphene oxide as sensing films. Sens. Actuators, B **191**, 779–783 (2014)
6. J. Xie, H. Wang, Y.H. Lin, Y. Zhou, Y.P. Wu, Highly sensitive humidity sensor based on quartz crystal microbalance coated with ZnO colloid spheres. Sens. Actuators, B **177**, 1083–1088 (2013)
7. Y. Yao, Y.J. Xue, Impedance analysis of quartz crystal microbalance humidity sensors based on nanodiamond/graphene oxide nanocomposite film. Sens. Actuators, B **211**, 52–58 (2015)
8. Y. Yao, X.D. Chen, W.M. Ma, W.W. Ling, Quartz crystal microbalance humidity sensors based on nanodiamond sensing films. IEEE Trans. Nanotechnol. **13**, 386–393 (2014)
9. F.X. Liang, L.B. Luo, L.X. Zheng, H. Cheng, Y.Y. Li, TiO₂ nanotube-based field effect transistors and their application as humidity sensors. Mater. Res. Bull. **47**, 54–58 (2012)
10. M. Zhuo, Y.J. Chen, J. Sun, H.M. Zhang, Humidity sensing properties of a single Sb doped SnO₂ nanowire field effect transistor. Sens. Actuators, B **186**, 78–83 (2013)
11. D. Jung, J. Kim, G.S. Lee, Enhanced humidity-sensing response of metal oxide coated carbon nanotube. Sens. Actuators, A **223**, 11–17 (2015)
12. S. Jung, T. Ji, ZnO nanorod-based humidity sensors with fast response. IEEE Electron. Device Lett. **35**, 960–962 (2014)
13. J.-L. Hou, C.-H. Wu, T.-J. Hsueh, Self-biased ZnO nanowire humidity sensor vertically integrated on triple junction solar cell. Sens. Actuators, B **197**, 137–141 (2014)

14. J. Herrán, I. Fernández, E. Ochoteco, G. Cabañero, H. Grande, The role of water vapour in ZnO nanostructures for humidity sensing at room temperature. Sens. Actuators, B **198**, 239–242 (2014)

15. Q.Q. Jia, H.M. Ji, Y. Zhang, Y.L. Chen, X.H. Sun, Z.G. Jin, Rapid and selective detection of acetone using hierarchical ZnO gas sensor for hazardous odor markers application. J. Hazard. Mater. **276**, 262–270 (2014)

16. S. Liu, B. Yu, H. Zhang, T. Fei, T. Zhang, Enhancing NO_2 gas sensing performances at room temperature based on reduced graphene oxide-ZnO nanoparticles hybrids. Sens. Actuators, B **202**, 272–278 (2014)

17. K.H. Kim, Z.G. Jin, Y. Abe, M. Kawamura, A comparative study on the structural properties of ZnO and Ni-doped ZnO nanostructures. Mater. Lett. **149**, 8–11 (2015)

18. C.S. Chen, X.D. Xie, G.J. Zhao, B. Zeng, X.T. Ning, S.Y. Cao, Y. Xiao, Y.P. Mei, X.M. Huang, Graphene/multi-walled carbon nanotube composite as an effective supports to enhance the photocatalytic property of Cu-doped ZnO nanopaticles. Funct. Mater. Lett. **6**, 1350062 (2013)

19. D. Zhang, N. Yin, B. Xia, Facile fabrication of ZnO nanocrystalline-modified graphene hybrid nanocomposite toward methane gas sensing application. J. Mater. Sci.: Mater. Electron. **26**, 5937–5945 (2015)

20. S. Biswas, G.P. Kar, D. Arora, S. Bose, A unique strategy towards high dielectric constant and low loss with multiwall carbon nanotubes anchored onto graphene oxide sheets. RSC Adv. **5**, 24132–24138 (2015)

21. H.D. Liu, Carbon nanotubes anchored with SnO_2 nanosheets as anode for enhanced Li-ion storage. J. Mater. Sci.: Mater. Electron. **25**, 3353–3357 (2014)

22. Y. Li, T.T. Wu, M.J. Yang, Humidity sensors based on the composite of multi-walled carbon nanotubes and crosslinked polyelectrolyte with good sensitivity and capability of detecting low humidity. Sens. Actuators, B **203**, 63–70 (2014)

23. X. Yun, J. Wang, L. Shen, H. Dou, X. Zhang, Three-dimensional graphene nanosheets/carbon nanotube paper as flexible electrodes for electrochemical capacitors. RSC Adv. **5**, 22173–22177 (2015)

24. J.G. Tait, M.F.L. De Volder, D. Cheyns, P. Heremans, B.P. Rand, Absorptive carbon nanotube electrodes: consequences of optical interference loss in thin film solar cells. Nanoscale **7**, 7259–7266 (2015)

25. S. Fu, G. Yang, Y. Zhou, H. Pan, C.M. Wai, D. Du, Y. Lin, Ultrasonic enhanced synthesis of multi-walled carbon nanotube supported Pt–Co bimetallic nanoparticles as catalysts for the oxygen reduction reaction. RSC Adv. **5**, 32685–32689 (2015)

26. T. Das, S. Banerjee, K. Dasgupta, J.B. Joshi, V. Sudarsan, Nature of the Pd–CNT interaction in Pd nanoparticles dispersed on multi-walled carbon nanotubes and its implications in hydrogen storage properties. RSC Adv. **5**, 41468–41474 (2015)

27. I. Dube, D. Jiménez, G. Fedorov, A. Boyd, I. Gayduchenko, M. Paranjape, P. Barbara, Understanding the electrical response and sensing mechanism of carbon-nanotube-based gas sensors. Carbon **87**, 330–337 (2016)

28. D. Zhang, J. Tong, B. Xia, Humidity-sensing properties of chemically reduced graphene oxide/polymer nanocomposite film sensor based on layer-by-layer nano self-assembly. Sens. Actuators, B **197**, 66–72 (2014)

29. C.L. Cao, C.G. Hu, L. Fang, S.X. Wang, Y.S. Tian, C.Y. Pan, Humidity sensor based on multi-walled carbon nanotube thin films. J. Nanomater. **2011**, 707303 (2011)

30. J. Lee, D. Cho, Y. Jeong, A resistive-type sensor based on flexible multi-walled carbon nanotubes and polyacrylic acid composite films. Solid-State Electron. **87**, 80–84 (2013)

31. F.S. Tsai, S.J. Wang, Shui-Jinn, Enhanced sensing performance of relative humidity sensors using laterally grown ZnO nanosheets. Sens. Actuators, B **193**, 280–287 (2014)

32. N.F. Hsu, M. Chang, C.H. Lin, Synthesis of ZnO thin films and their application as humidity sensors. Microsyst. Technol. **19**, 1737–1743 (2012)

33. D. Zhang, J. Liu, H. Chang, A. Liu, B. Xia, Characterization of a hybrid composite of SnO_2 nanocrystal-decorated reduced graphene oxide for ppm-level ethanol gas sensing application. RSC Adv. **5**, 18666–18672 (2015)

34. X.J. Chen, J. Zhang, Z.L. Wang, Q. Yan, S.C. Hui, Humidity sensing behavior of silicon nanowires with hexamethyldisilazane modification. Sens. Actuators, B **156**, 631–636 (2011)

35. Y. Wang, S. Park, J.T.W. Yeow, A. Langner, F. Müller, A capacitive humidity sensor based on ordered macroporous silicon with thin film surface coating. Sens. Actuators, B **149**, 136–142 (2010)

36. Y. Kim, B. Jung, H. Lee, H. Kim, K. Lee, H. Park, Capacitive humidity sensor design based on anodic aluminum oxide. Sens. Actuators, B **141**, 441–446 (2009)

37. G.H. Lu, L.E. Ocola, J.H. Chen, Reduced graphene oxide for room-temperature gas sensors. Nanotechnology **20**, 445502 (2009)

38. G.H. Lu, L.E. Ocola, J.H. Chen, Gas detection using low-temperature reduced graphene oxide sheets. Appl. Phys. Lett. **94**, 083111 (2009)

39. F. Barroso-Bujans, S. Cerveny, A. Alegra, J. Colmenero, Sorption and desorption behavior of water and organic solvents from graphite oxide. Carbon **48**, 3277–3286 (2010)

40. T. Fei, K. Jiang, F. Jiang, R. Mu, T. Zhang, Humidity switching properties of sensors based on multiwalled carbon nanotubes/polyvinyl alcohol composite films. J. Appl. Polym. Sci. **131**, 3972 (2014)